



## OPEN ACCESS

## EDITED BY

Trude Schwarzacher,  
University of Leicester, United Kingdom

## REVIEWED BY

Martin A. Lysak,  
Masaryk University, Czechia  
Steven Dreissig,  
Martin Luther University  
of Halle-Wittenberg, Germany

## \*CORRESPONDENCE

Andrea Pedrosa-Harand

✉ andrea.harand@ufpe.br;

André Marques

✉ amarques@mpipz.mpg.de

RECEIVED 31 October 2023

ACCEPTED 18 January 2024

PUBLISHED 07 February 2024

## CITATION

Mata-Sucre Y, Parteka LM, Ritz CM,  
Gatica-Arias A, Félix LP, Thomas WW,  
Souza G, Vanzela ALL, Pedrosa-Harand A  
and Marques A (2024) Oligo-barcode  
illuminates holocentric karyotype evolution  
in *Rhynchospora* (Cyperaceae).  
*Front. Plant Sci.* 15:1330927.  
doi: 10.3389/fpls.2024.1330927

## COPYRIGHT

© 2024 Mata-Sucre, Parteka, Ritz, Gatica-Arias,  
Félix, Thomas, Souza, Vanzela, Pedrosa-Harand  
and Marques. This is an open-access article  
distributed under the terms of the [Creative  
Commons Attribution License \(CC BY\)](#). The  
use, distribution or reproduction in other  
forums is permitted, provided the original  
author(s) and the copyright owner(s) are  
credited and that the original publication in  
this journal is cited, in accordance with  
accepted academic practice. No use,  
distribution or reproduction is permitted  
which does not comply with these terms.

# Oligo-barcode illuminates holocentric karyotype evolution in *Rhynchospora* (Cyperaceae)

Yennifer Mata-Sucre <sup>1,2</sup>, Letícia Maria Parteka <sup>1,3</sup>,  
Christiane M. Ritz <sup>4,5,6</sup>, Andrés Gatica-Arias <sup>7</sup>,  
Leonardo P. Félix <sup>8</sup>, William Wayt Thomas <sup>9</sup>,  
Gustavo Souza <sup>2</sup>, André L. L. Vanzela <sup>3</sup>,  
Andrea Pedrosa-Harand <sup>2\*</sup> and André Marques <sup>1\*</sup>

<sup>1</sup>Department of Chromosome Biology, Max Planck Institute for Plant Breeding Research, Cologne, Germany, <sup>2</sup>Laboratório de Citogenética e Evolução Vegetal, Departamento de Botânica, Centro de Biociências, Universidade Federal de Pernambuco, Recife, Brazil, <sup>3</sup>Laboratory of Cytogenetics and Plant Diversity, Department of General Biology, Londrina State University, Londrina, Brazil, <sup>4</sup>Department of Botany, Senckenberg Museum for Natural History Görlitz, Senckenberg – Member of the Leibniz Association, Görlitz, Germany, <sup>5</sup>Technical University Dresden, International Institute (IHI) Zittau, Chair of Biodiversity of Higher Plants, Zittau, Germany, <sup>6</sup>German Centre for Integrative Biodiversity Research (iDiv) Halle-Jena-Leipzig, Leipzig, Germany, <sup>7</sup>School of Biology, University of Costa Rica, San Pedro, Costa Rica, <sup>8</sup>Laboratory of Plant Cytogenetics, Department of Biosciences, Federal University of Paraíba, Areia, Brazil, <sup>9</sup>Institute of Systematic Botany, New York Botanical Garden, Bronx, NY, United States

Holocentric karyotypes are assumed to rapidly evolve through chromosome fusions and fissions due to the diffuse nature of their centromeres. Here, we took advantage of the recent availability of a chromosome-scale reference genome for *Rhynchospora breviuscula*, a model species of this holocentric genus, and developed the first set of oligo-based barcode probes for a holocentric plant. These probes were applied to 13 additional species of the genus, aiming to investigate the evolutionary dynamics driving the karyotype evolution in *Rhynchospora*. The two sets of probes were composed of 27,392 (green) and 23,968 (magenta) oligonucleotides (45-nt long), and generated 15 distinct FISH signals as a unique barcode pattern for the identification of all five chromosome pairs of the *R. breviuscula* karyotype. Oligo-FISH comparative analyzes revealed different types of rearrangements, such as fusions, fissions, putative inversions and translocations, as well as genomic duplications among the analyzed species. Two rounds of whole genome duplication (WGD) were demonstrated in *R. pubera*, but both analyzed accessions differed in the complex chain of events that gave rise to its large, structurally diploidized karyotypes with  $2n = 10$  or 12. Considering the phylogenetic relationships and divergence time of the species, the specificity and synteny of the probes were maintained up to species with a divergence time of ~25 My. However, karyotype divergence in more distant species hindered chromosome mapping and the inference of specific events. This barcoding system is a powerful tool to study chromosomal variations and genomic evolution in holocentric chromosomes of *Rhynchospora* species.

## KEYWORDS

beaksedges, chromosome rearrangements, chromosome fusion and fission, genome evolution, polyploidy, karyotype evolution, *Rhynchospora*

## Introduction

Despite their necessity for proper chromosome segregation, the organization of centromeres is diverse among eukaryotes (Drinnenberg and Akiyoshi, 2017). Based on their chromosomal localization, two main configurations are recognized: monocentromeres and holocentromeres, referring to the localized, size-restricted or the diffuse distribution of centromeric activity along the chromosome, respectively (Melters et al., 2012; Schubert et al., 2020; Wong et al., 2020). The peculiar diffuse structural organization of the latter allows spindle fibers to bind along the entire length of the so-called holocentric chromosomes. Thus, fragments originated from chromosomal breaks and fusions can be inherited during cell division more frequently compared to their monocentric counterparts (Vanzela and Colaço 2002; Melters et al., 2012; Heckmann and Houben 2013; Jankowska et al., 2015). In species with holocentric chromosomes, fusions and fissions do not appear to disrupt proper segregation, so holocentricity has been assumed to potentially reduce or eliminate selective pressure against chromosomal rearrangements, triggering reproductive isolation, i.e., chromosomal speciation (Lucek et al., 2022).

Holocentromeres have arisen several times independently among animals and plants, such as in the Cyperaceae (sedge) family (Melters et al., 2012; Escudero et al., 2016; Senaratne et al., 2022). The genus *Rhynchospora* Vahl (beaksedges) is the third largest genus of Cyperaceae (Araújo et al., 2012), with about 400 species distributed worldwide (POWO, 2023). Chromosomal numbers range from  $2n = 4$  in *R. tenuis* Link (Vanzela 1996) to  $2n = 61$  in *R. globosa* (Kunth) Roem. & Schult. (Burchardt et al., 2020), with a most likely ancestral chromosomal number (ACN) of  $x = 5$  (Burchardt et al., 2020; Hofstatter et al., 2022). Models of chromosomal evolution point to polyploidy as the main driver in *Rhynchospora*, followed by dysploidy (Ribeiro et al., 2018; Burchardt et al., 2020; Hofstatter et al., 2022). Recently, we described an auto-octoploid origin for *Rhynchospora pubera* (Vahl) Boeckeler ( $2n = 10$ ), formed after two rounds of genome duplication. Remarkably, post-polyploidy genome shuffling events due to end-to-end chromosome fusions substantially reduced its chromosome number to the ACN  $x = 5$ , demonstrating that extensive chromosomal rearrangements underlie rapid karyotype evolution in the genus (Hofstatter et al., 2022). Although chromosome fusions were independently observed in both *R. tenuis* ( $2n = 4$ ) and *R. pubera* ( $2n = 10$ ) (Hofstatter et al., 2022), changes in chromosome number were only observed in *R. tenuis*, where three end-to-end chromosome fusions explained its reduced karyotype from the ancestral  $n = 5$  to  $n = 2$ . Thus, it is likely that chromosomal rearrangements may still be hidden in species having the common ACN  $x = 5$ .

Whole genome comparison might be considered the most comprehensive way to shed light on chromosomal evolution. However, most plant groups still have only a single reference genome, making comparative genomic analyses between closely related species difficult and requiring the use of alternative feasible methods (Parween et al., 2015; Qin et al., 2019; Escudero et al., 2023). Chromosome barcoding with oligo-based probes has been

used to determine karyotypes and investigate chromosomal rearrangements, meiotic pairing, and recombination in a wide range of species (Braz et al., 2018; Meng et al., 2018; de Oliveira Bustamante et al., 2021; do Vale Martins et al., 2021; Li et al., 2021; Doležalová et al., 2022; Nascimento and Pedrosa-Harand, 2023). Oligo-FISH barcoding is based on the production of two different oligomer libraries from multiple regions of multiple chromosomes to produce a unique barcode signal pattern for each individual chromosome pair, facilitating the unambiguous identification of all chromosomes of a species in a single FISH experiment (Braz et al., 2018; Braz et al., 2020; de Oliveira Bustamante et al., 2021; Liu and Zhang, 2021). The availability of chromosome-scale reference genomes for *R. pubera*, *R. tenuis* and *R. breviscula* H. Pfeiff. (Hofstatter et al., 2022) provide the unique opportunity to design oligo-FISH probes for the creation of a universal oligo-FISH barcoding system to study genomic evolution in the genus *Rhynchospora*. Here we developed an oligo-FISH barcoding system based on *R. breviscula*, since it represents a truly diploid genome with the conserved ACN of the genus ( $x = 5$ ). Applying this oligo-barcode system comparatively across additional 13 species in the holocentric genus *Rhynchospora*, we detected a high degree of collinear regions among species of section *Dichromena* and further identified major chromosome structural changes in the genus. We demonstrate that the oligo-FISH-based barcode technique is a powerful tool for chromosome identification and karyotype evolution research even in highly dynamic holocentric karyotypes.

## Results

### Development of barcoding probes for chromosome identification in *Rhynchospora* species

We have developed two barcode-oligo probes (Rbv-I and Rbv-II) for chromosome identification in *Rhynchospora* species. These probes comprise 27,392 and 23,968 oligonucleotides (45-nt), respectively, which were identified in the five chromosomes of the *R. breviscula* reference genome (Hofstatter et al., 2022). The Rbv-I probe (green signals) covered 8 different regions, whereas the Rbv-II probe (magenta signals) covered 7 regions in the five *Rhynchospora* chromosomes (Figure 1A). Each probe covered between 585 and 1,110 kb of a chromosomal segment in the pseudomolecule and comprised around 3,424 oligonucleotides (Table 1). The oligo-FISH barcode libraries, hereafter referred to as oligo-probes, were designed to achieve a density between 4.13 and 4.19 oligos/kb in the region of interest to ensure good visibility of the hybridization signals after FISH (Table 1; Supplementary Table S1).

To validate the accuracy of the Rbv-I and Rbv-II oligo-probes, hybridizations of mitotic metaphase cells were performed in the same *R. breviscula* genotype used as the reference genome (Hofstatter et al., 2022). The green and magenta FISH probes generated bright and specific signals on all 10 homologous chromosomes, matching to the predicted patterns and validating the chromosome specificity of the oligo-probes (Figure 1B). The

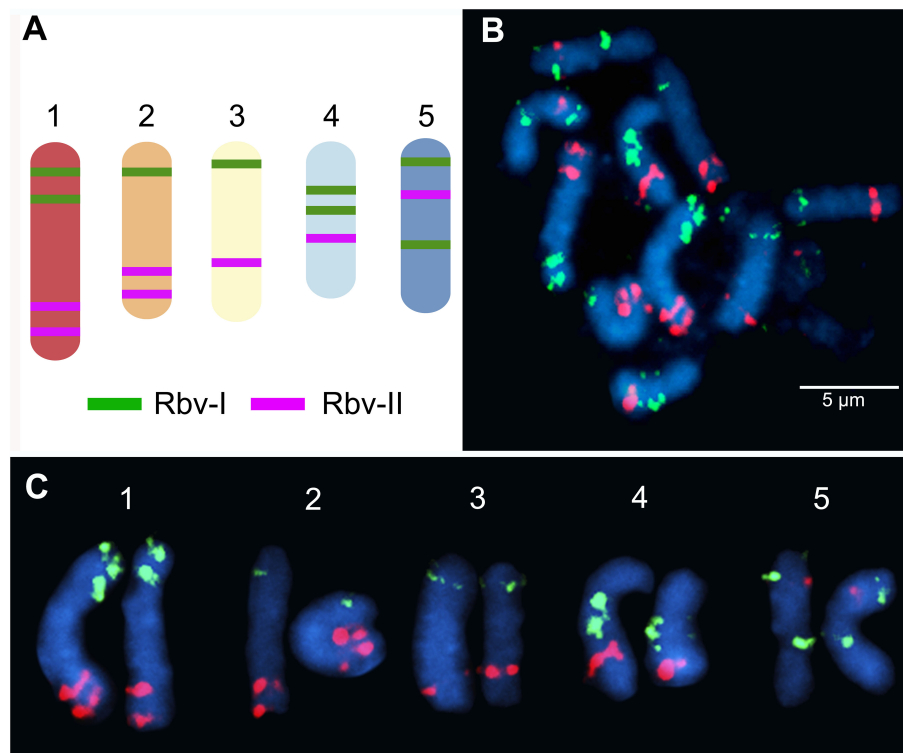


FIGURE 1

Predicted location and mapping of oligo-FISH barcode signals in *Rhynchospora breviuscula*. (A) Predicted oligos were selected from a total of 15 chromosomal regions (8 green "Rbv-I" and 7 magenta "Rbv-II" regions). The five chromosome pairs can be distinguished from each other based on the number and location of the Rbv-I/Rbv-II signals. (B) FISH mapping of metaphase mitotic chromosomes of *R. breviuscula* using oligo-barcode probes Rbv-I (green) and Rbv-II (magenta). (C) Karyogram identifying homologous chromosomes 1 to 5 from the same cells shown in (B) of *R. breviuscula*. Chromosomes were counterstained with DAPI (blue). Bar = 5  $\mu$ m.

TABLE 1 Genomic positions of oligo barcodes in the reference genome of *Rhynchospora breviuscula* (Rbv).

Chromosome	Total size (Mb)	Marker	Genome position		Region length in Kb
Rbv1	93.58	Rbv-I	3,145,145	4,041,370	896.23
		Rbv-I	15,415,340	16,488,297	1072.00
		Rbv-II	77,213,554	77,992,131	778.58
		Rbv-II	91,873,246	92,904,012	1030.77
Rbv2	74.03	Rbv-I	11,828,990	12,414,065	585.08
		Rbv-II	59,115,590	59,861,785	746.00
		Rbv-II	67,985,286	68,682,041	696.76
Rbv3	71.10	Rbv-I	6,095,377	6,980,542	885.17
		Rbv-II	53,557,881	54,188,768	630.89
Rbv4	69.90	Rbv-I	25,774,368	26,432,875	658.51
		Rbv-I	34,777,690	35,887,485	1109.80
		Rbv-II	49,042,597	49,847,722	805.13
Rbv5	68.82	Rbv-I	6,282,633	7,105,650	823.02
		Rbv-II	18,187,875	18,744,140	556.26
		Rbv-I	42,321,465	42,920,852	599.39

Total size and region's length were calculated using the available reference genome (Hofstatter et al., 2022). The color of each chromosome marker was defined in accordance with the Figure 1 description.

positions of the signals formed a barcode pattern that uniquely identified the five chromosome pairs of *R. breviuscula* (Figure 1C). The FISH signals of the Rbv-I probes (green) were weaker than those of the Rbv-II probe (magenta, Figure 1C).

## Comparative karyotype evolution within *Rhynchospora* species revealed by barcode oligo-FISH

After establishing the karyotype identification system of *R. breviuscula*, we performed comparative oligo-FISH on 13 additional *Rhynchospora* species using the two probes developed here to reveal karyotype evolution in the genus (Figure 2; Supplementary Figure S1). Our sampling comprised species of all main five clades of the genus according to their phylogenetic relationships (Costa et al., 2023), except for clade III. Karyotype analysis revealed holocentric chromosomes in all species analyzed, evident from the lack of primary constriction, with chromosome numbers ranging from  $2n = 4$  to  $2n = 26$  and chromosome sizes ranging from 1.10  $\mu\text{m}$  (*R. alba*) to 16.43  $\mu\text{m}$  (*R. pubera*; Supplementary Table S2). The two oligo-probes generated recognizable barcode signals in most species of clade IV, similar to the observed for *R. breviuscula*. The observed patterns allowed us to infer multiple chromosome fusions, putative inversions and translocations in different chromosomes of some species, revealing that intra- and interchromosomal rearrangements occurred during the divergence of species from clade IV (Figure 2; Supplementary Figure S1). The barcode patterns were, however, less evident in species of clades I, II and V, congruent to the phylogenetic distances among clades, and limiting the overall use of this set of probes for a broader karyotype analysis. Nevertheless, we have outlined the main chromosome rearrangements in the genus below.

### Clade IV – Section *Dichromena* (Michx.) Griseb.

The oligo-probes Rbv-I and Rbv-II were hybridized to the somatic chromosomes of five species of the section *Dichromena*, i.e., *R. breviuscula*, *R. colorata* (L.) H. Pfeiff., *R. nervosa* (Vahl) Boeckeler ssp. *ciliata* (G. Mey.) T. Koyama, and *R. radicans* (Schltdl. & Cham.) H. Pfeiff.; as well as two accessions of *R. pubera*, our reference genotype with  $2n = 10$  (Hofstatter et al., 2022) and a recently collected accession with  $2n = 12$ , referred to here as “*R. pubera*-10” and “*R. pubera*-12”, respectively (Figures 2, 3). Green and magenta signals derived from the two probes confirmed our recent findings (Hofstatter et al., 2022) that the *R. pubera*-10 karyotype has originated from two rounds of whole genome duplication followed by a complex chain of end-to-end chromosome fusion events. Indeed, we observed a signal pattern congruent with four copies of each of the five chromosomes of *R. breviuscula* (Figures 2, 3A; Supplementary Figure S2). The *R. pubera*-12 accession was initially thought to be a dysploid cytotype of *R. pubera*-10 due to a single fission of one

chromosome pair. Nevertheless, our detailed analysis revealed a much more complex karyotype. We found this accession to have additional rearrangements besides the genome duplications and fusions found in *R. pubera*-10, as indicated from the FISH signal patterns observed from its six homologous chromosomes. The FISH pattern observed in *R. pubera*-12 suggests fission of one chromosome pair and loss of significant chromosomal regions likely due to massive genomic reshuffling (Figures 2, 3B). Although the quality of the FISH signals was similar to those of *R. breviuscula*, we could not find a pattern that allowed us to decipher its complex karyotype. Indeed, we could only count a total of 43 FISH signals, 21 of the Rbv-I probe and 22 of the Rbv-II probe, in contrast to the 60 signals observed in *R. pubera*-10 (Figures 3A, B). Even though a resolution/condensation matter could be hiding additional visualization of signals, these findings are consistent with the loss of multiple genomic regions equivalent to a set of *R. breviuscula* chromosomes during the karyotype evolution of *R. pubera*-12 (Figure 2).

Hybridization signals of Rbv-I and Rbv-II oligoprobes on the chromosomes of *R. colorata* ( $2n = 10$ ), *R. nervosa* ssp. *ciliata* ( $2n = 10$ ), and *R. radicans* ( $2n = 10$ ) matched exactly the same pattern as those of *R. breviuscula*, indicating a high synteny and collinearity among species with same ploidy and chromosome number in the section *Dichromena* (Figure 2; Supplementary Figure S1).

### Clade IV – Section *Tenues* Kük

Species of this section, *R. tenuis*, *R. riparia* (Nees) Boeckeler, *R. filiformis* Vahl and *R. tenerrima* Nees ex Spreng., presented rearranged patterns of signals for Rbv-I and Rbv-II oligoprobes, showing fusions, inversions, translocations and duplications with respect to the *R. breviuscula* pattern (Figures 2, 4). A putative intrachromosomal translocation and a duplication was observed on chromosome 2 of *R. filiformis* ( $2n = 10$ ; Figure 4B), in which one of the magenta signals translocated closer to the opposite end of the chromosome adjacent to the green signal, which is duplicated, different from that observed in the *R. breviuscula* pattern. A large inversion on chromosome 1 of *R. riparia* ( $2n = 10$ ) would explain the changes observed in the FISH signal pattern (Figure 4C). Duplication and deletion of magenta or green oligo-barcode signals were also observed on chromosome 5 of *R. filiformis* and *R. riparia*, indicating additional small structural rearrangements in these species (Figures 4B, C). *Rhynchospora tenuis* ( $2n = 4$ ; Figure 4D) showed all the FISH signal patterns of the five *R. breviuscula* chromosomes on its two chromosome pairs, except for a putative inversion on chromosome 2, confirming the fusion events of chromosomes 1-2-5 and 3-4 on its chromosomes 1 and 2, respectively (Figure 4D), as we have recently shown by genome assembly (Hofstatter et al., 2022). Another interesting case is found in *R. tenerrima*, a species with  $2n = 20$ , which is assumed to be a polyploid (Arguelho et al., 2012). The hybridization pattern of Rbv-I and Rbv-II FISH probes revealed 21 signals in total (11 green and 10 magenta, Figure 4E), in contrast to the expected 15 for a diploid if compared to *R. breviuscula* chromosomes. Thus, it is possible for this species to be polyploid, but due to the reduced number of

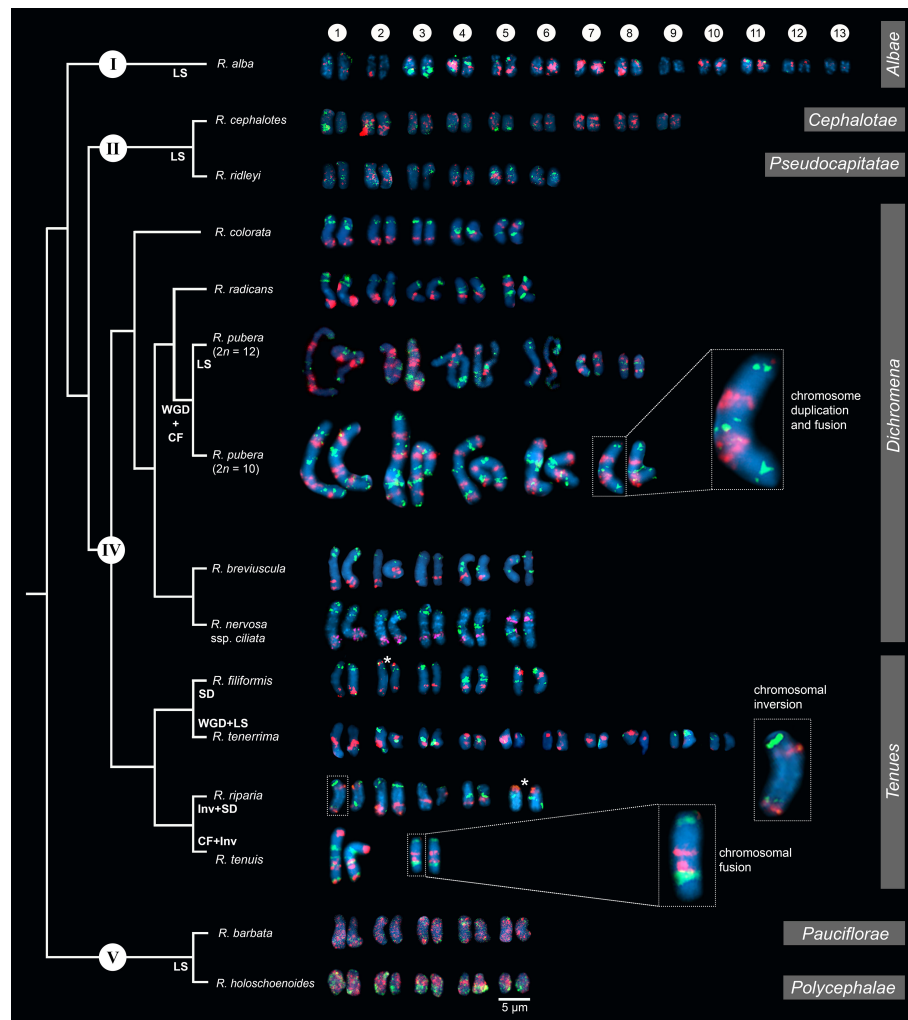


FIGURE 2

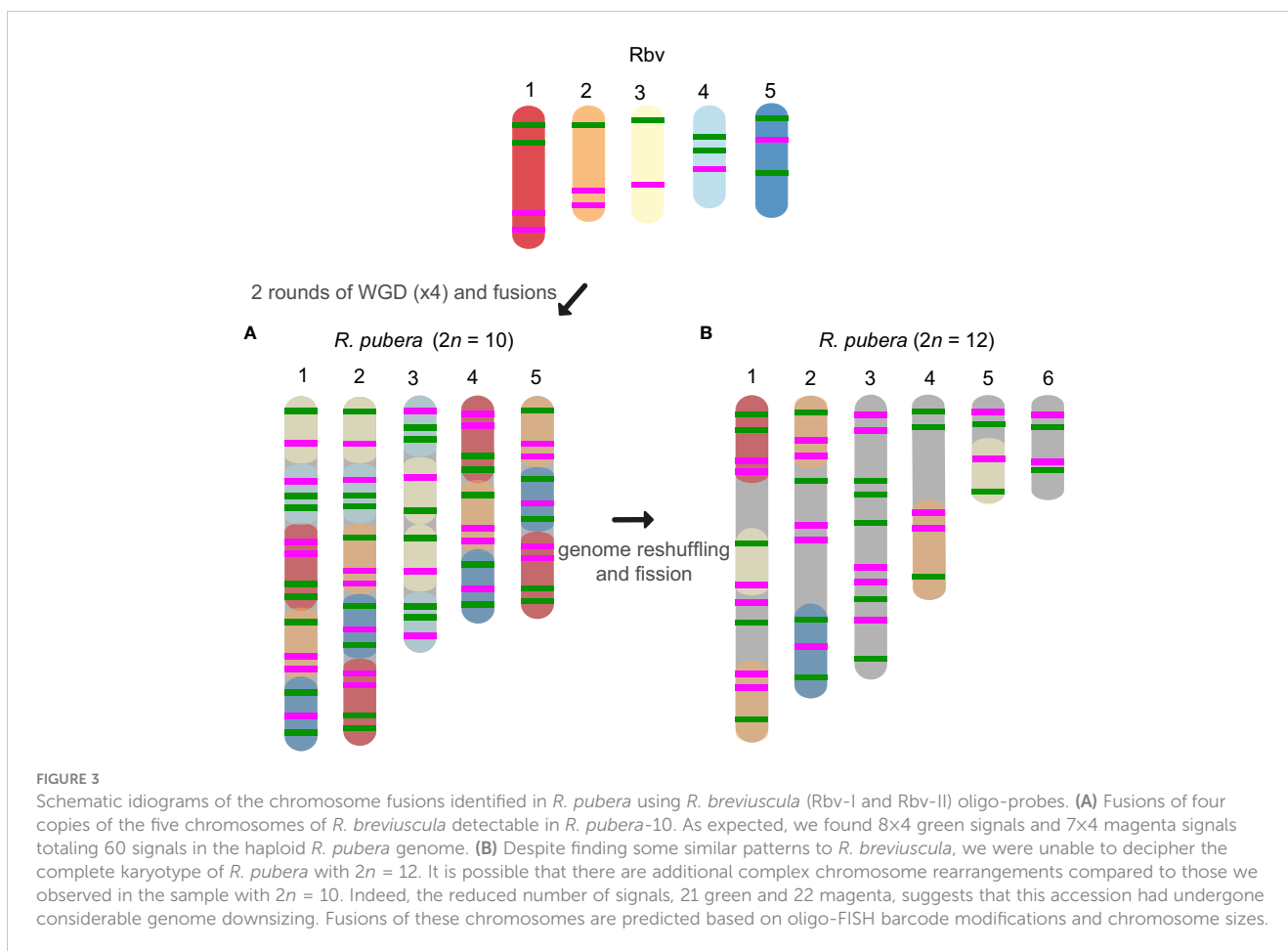
Comparative karyograms of 14 *Rhynchospora* species based on the barcode oligo-probes Rbv-I (green) and Rbv-II (magenta). For each species, chromosome pairs are ordered from left to right according to their putative *R. breviuscula* orthologs. Insets illustrate chromosome fusions in *R. pubera* and *R. tenuis*, and an inversion in chr1 in *R. riparia*. Asterisk points to signal duplication in chr2 and chr5 of *R. filiformis* and *R. riparia*, respectively, likely due to chromosomal translocations. For species without clear oligo-probe patterns, chromosome pairs were arranged according to their decreasing sizes. CF indicates chromosome fusion events; Inv refers to inversions, LS refers to loss of signal (deletions), while SD refers to signal duplications. WGD denotes whole genome duplication. Clade numbering and phylogenetic relationships are based on Costa et al. (2023). Section assignments (grey bars on the right) are given based on recent phylogenetic and taxonomic revisions (Thomas et al., 2009; Buddenhagen, 2016; Silva Filho et al., 2021). Bar = 5 µm.

signals expected for a fully duplicated set of chromosomes, i.e., 30, *R. tenerrima* is likely already experiencing diploidization through genome downsizing. Indeed, this is evidenced from the lack of a similar barcode pattern in *R. breviuscula* chromosomes, which prevented us from deciphering its karyotype (Figure 4E).

## Other clades

In comparison to *R. breviuscula*, the rest of the species analyzed here diverged from a common ancestor ~35 Mya ago (Costa et al., 2023). The two oligo-probes produced massive background signals on the chromosomes of *R. holoschoenoides* (Rich.) Herter (sect. *Polycephalae* C.B. Clarke) and *R. barbata* (Vahl) Kunth (sect.

*Pauciflorae* Kük.; Figures 2, 5; Supplementary Figure S1), suggesting loss of sequence specificity or, less likely, extensive microcollinearity breaks between the genomes. On the other hand, signals were observed on the chromosomes of *R. alba* (sect. *Albae*), *R. cephalotes* (sect. *Cephalotae*) and *R. ridleyi* (sect. *Pseudocapitatae* Figures 2, 5), in congruence with closer phylogenetic distances. However, most of the chromosomes could not be clearly identified based on the barcode pattern observed in *R. breviuscula* chromosomes. The karyotypes of these species have higher chromosome numbers compared to *R. breviuscula*, up to 13 pairs in *R. alba*. Although the low number of hybridization signals observed for these species could indicate partial sequence divergency, it might also suggest that they have undergone chromosome fissions rather than polyploidy.

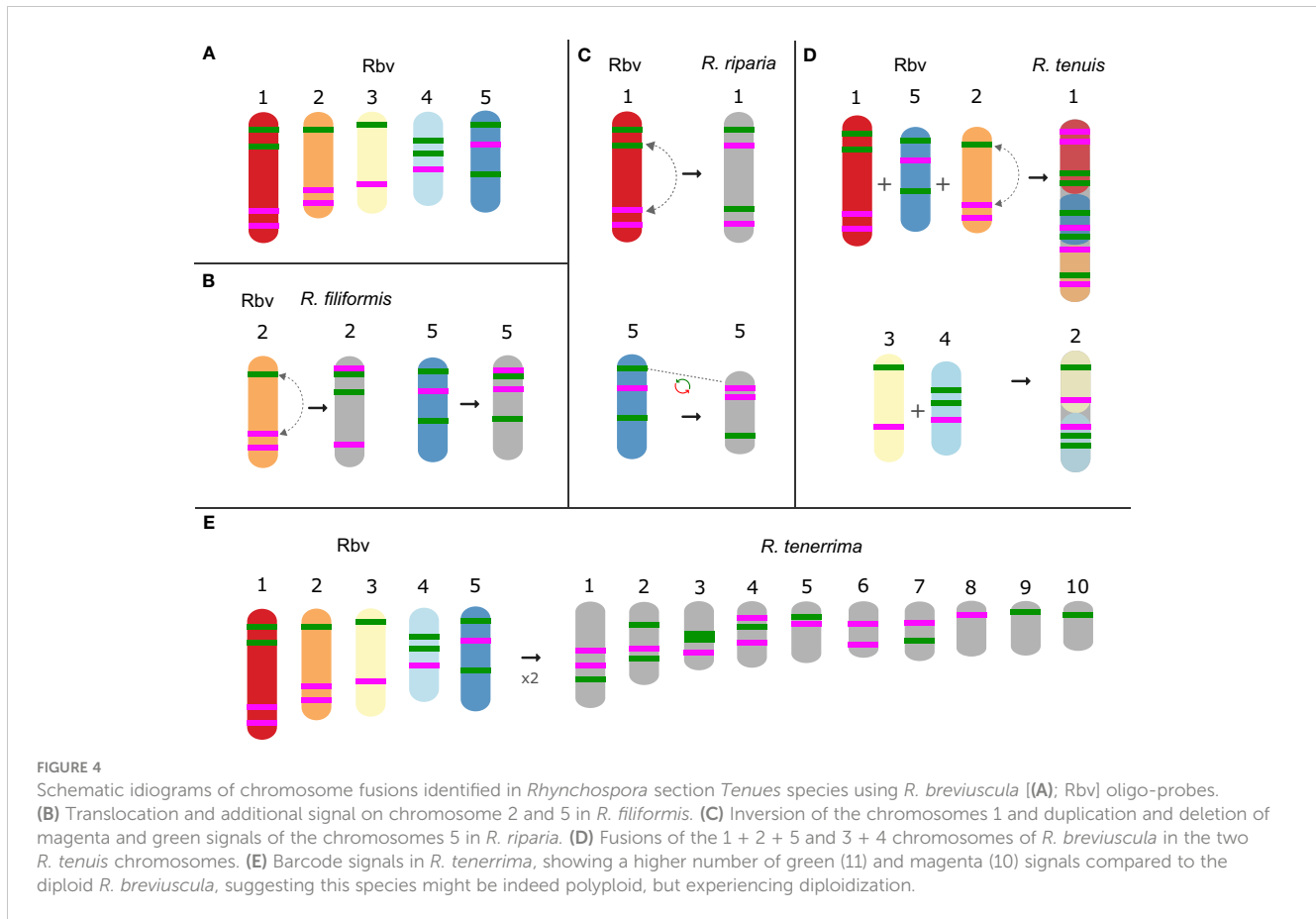


## Discussion

An optimized oligo-FISH painting method by *de novo* synthesis of thousands of oligos is now possible for species with assembled genomes, providing a powerful tool for understanding the structure, organization, and evolution of plant chromosomes (Braz et al., 2018; Liu et al., 2020; do Vale Martins et al., 2021; Li et al., 2021). Furthermore, oligo-FISH barcoding has also proven to be a powerful and efficient technique for chromosome identification and inference of intrachromosomal rearrangements that are not detected by chromosome painting (Braz et al., 2018; de Oliveira Bustamante et al., 2021; Luo et al., 2022; Nascimento and Pedrosa-Harand, 2023). Here we have successfully developed two sets of oligo-probes based on conserved regions with >20,000 oligos of 45 nt per linkage group, and applied oligo-FISH barcoding to identify all chromosome pairs in *R. breviuscula* karyotype. Among the genus *Rhynchospora*, only three species possess a published genome (Hofstatter et al., 2022) and of those, only *R. breviuscula* is a diploid with  $2n = 10$  chromosomes (reflecting its basic chromosome number  $x = 5$ ; Burchardt et al., 2020), making it the perfect candidate to develop the oligo-probes and transfer them into other species of *Rhynchospora*. We tested the barcode probes in 13 additional species of the genus, which represented seven of the 28 formally described sections (Thomas et al., 2009; Buddenhagen, 2016; Silva Filho et al., 2021).

In holocentric species, multiple chromosome rearrangements, mainly fusion and fission events, have been shown to be the main driver of their karyotype evolution and may exhibit adaptive potential possibly allowing chromosomal speciation (Hofstatter et al., 2022; Lucek et al., 2022; Senaratne et al., 2022; Escudero et al., 2023; Márquez-Corro et al., 2023). In fact, comparisons using recent available chromosome-scale genome assemblies between holocentric *Carex* and *Rhynchospora* species, as well as with their closest monocentric relative *Juncus* L. (rushes) have revealed conserved synteny despite high rates of chromosome fission and fusion in sedges (Hofstatter et al., 2022; Escudero et al., 2023). These data suggest high synteny conservation despite the ancient lineage split between rushes and sedges (>60 Mya) and between *Carex* and *Rhynchospora* (40–50 Mya; Hofstatter et al., 2022; Costa et al., 2023). In addition, the recently described chromosome fusions in the genomes of *R. pubera* and *R. tenuis* (Hofstatter et al., 2022) could now be confirmed by our oligo barcode probes, showing that this approach is also useful for dynamic holocentric karyotypes. Furthermore, we could detect the chromosomes involved in end-to-end fusions in *R. tenuis* ( $2n = 4$ ), as well as the two rounds of whole genome duplication events and the complex chain of end-to-end fusions that drove the karyotype evolution in *R. pubera* (Hofstatter et al., 2022).

Our oligo barcode analysis further allowed us to better understand an ongoing karyotype differentiation among different

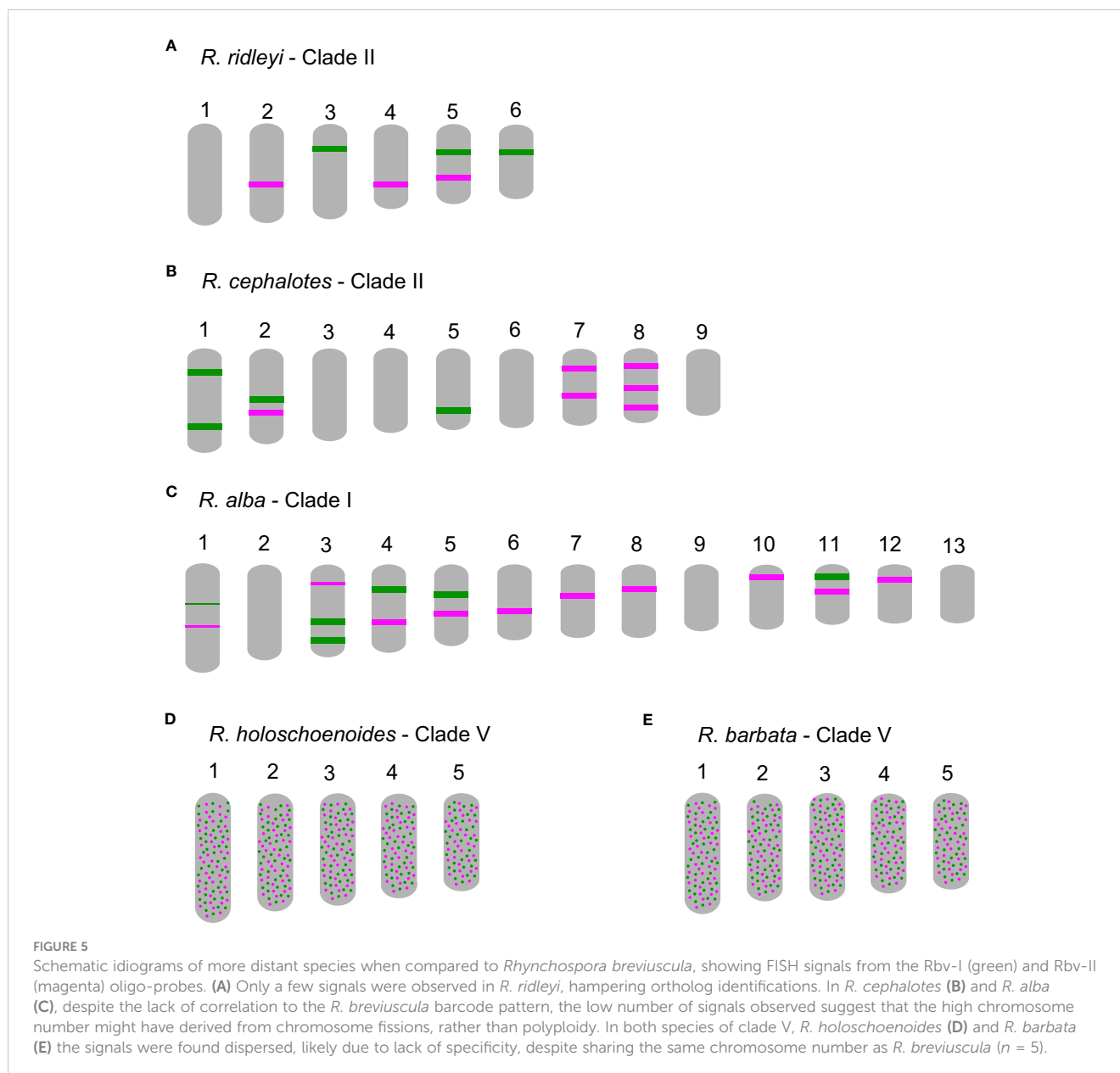


populations of *R. pubera*. Our reference *R. pubera* ( $2n = 10$ ) from the Brazilian northeast (Hofstatter et al., 2022) is the most common cytotype found for this species, but earlier studies have reported a population from Manaus, in the state of Amazonas in Northern Brazil, with  $2n = 12$  (Arguelho et al., 2012). Here, we report a newly collected sample from another population from Northern Brazil, from Belém in the state of Pará, also showing  $2n = 12$ . The oligo barcode pattern observed in *R. pubera*-12 indicates that its chromosomes originated from the same duplication and fusions events as observed in *R. pubera*-10, but also suggests ongoing complex chromosome genome reshuffling, leading to the ascending dysploidy, in a likely scenario of ongoing chromosomal speciation. Apparently, in contrary to the conservation of all four copies in the “standard” *R. pubera* karyotype, this accession has lost sequences corresponding to approximate one whole set of ancestral chromosomes. Such complex rearrangements are supported by the meiotic irregularities previously reported for a *R. pubera* cytotype with  $2n = 12$  (Arguelho et al., 2012). However, the limitations of the barcode probes, particularly when some signals were lost during genome reshuffling, underscore the need for a comprehensive genomic study to validate these findings.

Dual-color oligo-FISH is useful for studying species evolution and previous research has shown that oligo probes can be applied to chromosome identification in related species that diverged ~5 My ago, such as *Phaseolus* (Nascimento and Pedrosa-Harand, 2023), ~12

Mya as in *Cucumis* (Hans et al., 2015) or *Sorghum* (Yu et al., 2021), ~15 Mya as in *Solanum* species (Braz et al., 2018), ~18 Mya as in *Saccharum* (Yu et al., 2021) or even up to 45-55 Mya across different palm species (Zaki et al., 2021). Here we transferred *R. breviuscula* oligo-probes and demonstrated their utility for correct ortholog identification among species with divergence times up to ~25 My (clade IV, sections *Dichromena* and *Tenues*). Indeed, all true diploid species of sect. *Dichromena* with  $n = 5$  (*R. colorata*, *R. nervosa* and *R. radicans*) showed exactly the same barcode pattern as *R. breviuscula*. Similarly, species of the related sect. *Tenues* showed a very similar pattern, but with the occurrence of several recognizable rearrangements, e.g., fusions, inversions and translocations. Additionally, we could also detect a potential polyploidy event in *R. tenerrima*. However, the reduced number of signals observed in contrast to the expected duplicated amount of barcode signals suggest that this species is undergoing rediploidization. Indeed, no meiotic irregularities was reported for *R. tenerrima*, where a normal pollen development was observed (Arguelho et al., 2012). Low sequence similarity or the interruption of synteny have hampered the barcode recognition between species with divergence time up to ~30 My from *R. breviuscula*.

In general, our results indicate a strong relationship between chromosomal rearrangements and the current understanding of the phylogenetic relationships in *Rhynchospora*. Our oligo barcode results confirmed, as observed in other sedges: (i) there is high synteny among



holocentric genomes during long periods of time; (ii) that in the genus *Rhynchospora*, the ACN  $x = 5$  may be either conserved or a result of fusions and genomic reshuffle events; and (iii) that chromosome rearrangements after fission events appear to govern karyotypic diversity in the genus. The stasis of diploid karyotypes with  $2n = 10$  contrasts with the multiple rearrangements associated to, but not directly involved, in the dysploidy events, as also observed in monocentrics (Nascimento and Pedrosa-Harand, 2023). Ultimately, the current oligo-probe sets enabled the direct visualization of homologous regions on *Rhynchospora* chromosomes through a straightforward experimental method. These innovative oligo-barcode-based comparative FISH studies offer a potent instrument for illuminating the evolutionary dynamics of holocentric beaksedge genomes. This toolset can be readily employed to pinpoint additional *Rhynchospora* karyotypes resulting from chromosome fusion, fission, or polyploidy events, thereby unveiling potential chromosomal reorganization within evolutionarily divergent genomes.

## Materials and methods

### Plant material

Samples from *R. breviuscula*, *R. cephalotes*, *R. nervosa* ssp. *ciliata*, *R. pubera* ( $2n = 10$ ) and *R. tenuis* were already available from previous studies (Hofstatter et al., 2022; Ribeiro et al., 2017; Costa et al., 2021). The *R. colorata* (L.) H.Pfeiff. sample was commercially acquired. Additional nine samples from nine species were collected from different localities in Brazil, Costa Rica and Germany (Supplementary Table S3) and further cultivated under controlled greenhouse conditions (16h daylight, 26°C, >70% humidity) at the Max Planck Institute for Plant Breeding Research in Germany. Sampling includes *Rhynchospora alba* (L.) Vahl (Germany, Sachsen, Dauban, Großer Zug; bog), *R. barbata* (Vahl) Kunth (Areia-PB, Brazil), *R. filiformis* Vahl (Baía da Traição-PB, Brazil), *R. holoschoenoides* (Rich.) Herter (Baía da

Traição-PB, Brazil), *R. pubera* (Vahl) Boeckeler accession with  $2n = 12$  (Belém-PA, Brazil), *R. radicans* (Schltdl. & Cham.) H.Pfeiff. (San José, Costa Rica), *R. ridleyi* C.B. Clarke (Areia-PB, Brazil), *R. riparia* (Nees) Boeckeler (Rio Tinto-PB, Brazil), *R. tenerrima* Nees ex Spreng. (Vale do Codó-PR, Brazil) and *R. tenuis* Link (Ipojuca-PE, Brazil). These taxa represent species in the sections *Albae*, *Dichromena*, *Cephalotae*, *Pauciflorae*, *Polycephalae*, *Pseudocapitatae* and *Tenuis* (Thomas et al., 2009; Buddenhagen, 2016; Silva Filho et al., 2021).

## Oligo probe design

Oligo-FISH barcode probes were designed against the chromosome-scale sequence assembly of *R. breviuscula* (Hofstatter et al., 2022) using Daicel Arbor Biosciences' proprietary software (Daicel Arbor Bioscience, Ann Arbor, MI, USA). Briefly, target sequences were fragmented into 43–47 nucleotide-long overlapping probe candidate sequences that were compared to the rest of the genome sequence to exclude any candidates with potential cross-hybridization based on a predicted  $T_m$  of hybridization. Non-overlapping target-specific oligonucleotides were selected for the final probe sets and synthesized as myTAGs<sup>®</sup> Labeled Libraries (Daicel Arbor Bioscience). Target regions were selected with a relatively high density of oligos based on the density distribution profile on the entire chromosome (Supplementary Table S1), and then taking into account the regions conserved with *R. pubera* and *R. tenuis* chromosome-scale sequence assemblies (Hofstatter et al., 2022). The two libraries consist of ~ 20,000 oligomers each (45nt long) corresponding to eight green (Rbv-I) and seven magenta (Rbv-II) signals. Each chromosome of *R. breviuscula* has two to four unique signals, with specific combinations of green and magenta signals covering specific chromosomes regions (Figure 1). The libraries were synthesized by Arbor Biosciences (Ann Arbor, Michigan, USA) and directly labeled with Cy3 and Alexa-488 (Eurofins Genomics, Ebersberg, Germany).

## Chromosome spreads and oligo-fluorescence *in situ* hybridization

To prepare mitotic metaphase chromosomes, root tips were fixed in ethanol:acetic acid (3:1 v/v) for 2–24 h at room temperature and stored at  $-20^{\circ}\text{C}$ . Fixed root tips were washed twice in distilled water and digested in an enzymatic solution of 2% (w/v) cellulase (Onozuka)/20% (v/v) pectinase (Sigma) at  $37^{\circ}\text{C}$ , for 90 min. Meristems were macerated in a drop of 45% acetic acid and spread on a hot plate following Ruban et al. (2014). Oligo-FISH was performed according to the protocol proposed by Braz et al. (2020) with some modifications. The hybridization mixture consisted of 50% formamide,  $2\times\text{SSC}$  (sodium citrate saline; pH 7.0), 10% dextran, 350 ng of Alexa-labeled probe and 200 ng of Cy3-labeled probe, in a total volume of 10  $\mu\text{l}$  per slide. Chromosomes

were denatured for 5–7 min at  $75^{\circ}\text{C}$  and incubated for 18–24 h at  $37^{\circ}\text{C}$  in a humid chamber. Subsequently, coverslips were gently removed and the slides were washed with  $2\times$  and  $0.1\times$  SSC at  $42^{\circ}\text{C}$  (~ 76% final stringency). In addition, low-stringency baths were also performed in more distant species, following Braz et al. (2020). Chromosomes were counterstained with 2  $\mu\text{g}/\text{mL}$  DAPI in Vectashield solution (Vector Laboratories).

## Image processing and comparative analyses

Images of the chromosomes were captured with a Zeiss Axiovert 200M microscope equipped with a Zeiss AxioCam CCD. Images were analyzed using the ZEN software (Carl Zeiss GmbH, Jena Germany). Karyograms were obtained from the best cell photographed using Adobe Photoshop CS5 (version 12.0) and ordered following their orthologies. Chromosome size measurements of the 14 species studied (Supplementary Table S2) were constructed after analysis of at least five whole metaphase cells using DRAWID 0.26 software (Kirov et al., 2017) and interpreted using the genetic relationships described in Costa et al. (2023).

## Data availability statement

The original data presented in the study are included in the article/Supplementary Files. Further inquiries can be directed to the corresponding authors.

## Author contributions

YM-S: Formal analysis, Investigation, Methodology, Visualization, Writing – original draft, Writing – review & editing. LMP: Formal analysis, Investigation, Methodology, Writing – review & editing. CMR: Data curation, Writing – review & editing. AG-A: Data curation, Writing – review & editing. LPF: Data curation, Writing – review & editing. WWT: Data curation, Writing – review & editing. GS: Supervision, Visualization, Writing – review & editing. ALLV: Supervision, Visualization, Writing – review & editing. AP-H: Conceptualization, Funding acquisition, Supervision, Writing – original draft, Writing – review & editing. AM: Conceptualization, Funding acquisition, Investigation, Resources, Supervision, Writing – original draft, Writing – review & editing.

## Funding

The author(s) declare financial support was received for the research, authorship, and/or publication of this article. This work was conducted during a PhD sandwich fellowship awarded to YM-S and LP supported by the International Cooperation Program PROBRAL from CAPES – Brazilian Federal Agency for Support

and Evaluation of Graduate Education within the Ministry of Education of Brazil. This work was supported by a grant awarded to AP-H (PROBRAL CAPES/DAAD project number 88881.144086/2017-01) and CAPES code 001. GS receive a productivity fellowship from CNPq (process numbers PQ-312852/2021-5). AM thanks to the Max Planck Society and Deutsche Forschungsgemeinschaft (DFG, grant number MA 9363/3-1) for financial support.

## Acknowledgments

We acknowledge the excellent technical assistance of Christina Philipp and Ursula Pfordt for keeping the plants growing in the greenhouse at the MPIPZ. We thank the administration of the Biosphere Reserve “Oberlausitzer Heide- und Teichlandschaft” for providing occurrence information and sampling permit for *R. alba*.

## Conflict of interest

The authors declare that the research was conducted in the absence of any commercial or financial relationships that could be construed as a potential conflict of interest.

The author(s) declared that they were an editorial board member of Frontiers, at the time of submission. This had no impact on the peer review process and the final decision.

## References

- Araújo, A. C., Longhi-Wagner, H. M., and Thomas, W. W. (2012). A synopsis of *Rhynchospora* sect. *Pluriflorae* (Cyperaceae). *Brittonia* 64, 381–393. doi: 10.1007/s12228-012-9252-2
- Arguelho, E. G., Michelan, V. S., Nogueira, F. M., Da Silva, C. R. M., Rodriguez, C., Trevisan, R., et al. (2012). New chromosome counts in Brazilian species of *Rhynchospora* (Cyperaceae). *Caryologia* 65 (2), 140–146. doi: 10.1080/00087114.2012.711675
- Braz, G. T., He, L., Zhao, H., Zhang, T., Semrau, K., Rouillard, J. M., et al. (2018). Comparative oligo-FISH mapping: an efficient and powerful methodology to reveal karyotypic and chromosomal evolution. *Genetics* 208 (2), 513–523. doi: 10.1534/genetics.117.300344
- Braz, G. T., Yu, F., do Vale Martins, L., and Jiang, J. (2020). Fluorescent *in situ* hybridization using oligonucleotide-based probes. *In Situ Hybridization. Protoc.*, 71–83. doi: 10.1007/978-1-0716-0623-0\_4
- Buddenhagen, C. E. (2016). *A view of Rhynchosporae (Cyperaceae) diversification before and after the application of anchored phylogenomics across the angiosperms* (Tallahassee: Florida State University; Doctoral thesis).
- Burchardt, P., Buddenhagen, C. E., Gaeta, M. L., Souza, M. D., Marques, A., and Vanzela, A. L. (2020). Holocentric karyotype evolution in *Rhynchospora* is marked by intense numerical, structural, and genome size changes. *Front. Plant Sci.* 11, 536507. doi: 10.3389/fpls.2020.536507
- Costa, L., Marques, A., Buddenhagen, C., Thomas, W. W., Huettel, B., Schubert, V., et al. (2021). Aiming off the target: recycling target capture sequencing reads for investigating repetitive DNA. *Ann. Bot.* 128, 835–848. doi: 10.1093/aob/mcab063
- Costa, L., Marques, A., Buddenhagen, C. E., Pedrosa-Harand, A., and Souza, G. (2023). Investigating the diversification of holocentromeric satellite DNA *Tyba* in *Rhynchospora* (Cyperaceae). *Ann. Bot.* 131, 813–825. doi: 10.1093/aob/mcad036
- de Oliveira Bustamante, F., do Nascimento, T. H., Montenegro, C., Dias, S., do Vale Martins, L., Braz, G. T., et al. (2021). Oligo-FISH barcode in beans: A new chromosome identification system. *Theor. Appl. Genet.* 134, 3675–3686. doi: 10.1007/s00122-021-03921-z
- Doležalová, A., Sládeková, L., Šimoníková, D., Holušová, K., Karafiátová, M., Varshney, R. K., et al. (2022). Karyotype differentiation in cultivated chickpea revealed by Oligopainting fluorescence *in situ* hybridization. *Front. Plant Sci.* 12, 791303. doi: 10.3389/fpls.2021.791303
- do Vale Martins, L., de Oliveira Bustamante, F., da Silva Oliveira, A. R., da Costa, A. F., de Lima Feitoza, L., Liang, Q., et al. (2021). BAC-and oligo-FISH mapping reveals chromosome evolution among *Vigna angularis*, *V. unguiculata*, *Phaseolus vulgaris*. *Chromosoma* 130 (2-3), 133–147. doi: 10.1007/s00412-021-00758-9
- Drinnenberg, I. A., and Akiyoshi, B. (2017). Evolutionary lessons from species with unique kinetochores. *Prog. Mol. Subcell. Biol.* 56, 111–138. doi: 10.1007/978-3-319-58592-5\_5
- Escudero, M., Marques, A., Lucek, K., and Hipp, A. L. (2023). Genomic hotspots of chromosome rearrangements explain conserved synteny despite high rates of chromosome evolution in a holocentric lineage. *Mol. Ecol.* 00, 1–12. doi: 10.1111/mec.17086
- Escudero, M., Márquez-Corro, J. I., and Hipp, A. L. (2016). The phylogenetic origins and evolutionary history of holocentric chromosomes. *Syst. Bot.* 41 (3), 580–585. doi: 10.1600/036364416X692442
- Han, Y., Zhang, T., Thammapichai, P., Weng, Y., and Jiang, J. (2015). Chromosome-specific painting in *Cucumis* species using bulked oligonucleotides. *Genetics* 200 (3), 771–779. doi: 10.1534/genetics.115.177642
- Heckmann, S., and Houben, A. (2013). “Holokinetic centromeres”. *Plant centromere Biol.* (New York) 1, 83–94. doi: 10.1002/9781118525715
- Hofstätter, P. G., Thangavel, G., Lux, T., Neumann, P., Vondrak, T., Novak, P., et al. (2022). Repeat-based holocentromeres influence genome architecture and karyotype evolution. *Cell* 185 (17), 3153–3168. doi: 10.1016/j.cell.2022.06.045
- Jankowska, M., Fuchs, J., Klocke, E., Fojtová, M., Polanská, P., Fajkus, J., et al. (2015). Holokinetic centromeres and efficient telomere healing enable rapid karyotype evolution. *Chromosoma* 124, 519–528. doi: 10.1007/s00412-015-0524-y
- Kirov, I., Khrustaleva, L., Van Laere, K., Soloviev, A., Meeus, S., Romanov, D., et al. (2017). DRAWID: user-friendly java software for chromosome measurements and idiogram drawing. *Comp. Cytogenet.* 11 (4), 747. doi: 10.3897/compcytogen.v11i4.20830
- Li, G., Zhang, T., Yu, Z., Wang, H., Yang, E., and Yang, Z. (2021). An efficient Oligo-FISH painting system for revealing chromosome rearrangements and polyploidization in *Triticaceae*. *Plant J.* 105 (4), 978–993. doi: 10.1111/tpj.15081

## Publisher’s note

All claims expressed in this article are solely those of the authors and do not necessarily represent those of their affiliated organizations, or those of the publisher, the editors and the reviewers. Any product that may be evaluated in this article, or claim that may be made by its manufacturer, is not guaranteed or endorsed by the publisher.

## Supplementary material

The Supplementary Material for this article can be found online at: <https://www.frontiersin.org/articles/10.3389/fpls.2024.1330927/full#supplementary-material>

### SUPPLEMENTARY FIGURE 1

Chromosome identification by oligo-FISH barcoding in *Rhynchospora* species using Rbv-I (green) and Rbv-II (magenta) oligo probes developed based on *R. brevisuscula* ( $n = 5$ ) reference genome. *R. barbata*  $2n = 10$ , *R. holoschoenoides*  $2n = 10$ , *R. ridleyi*  $2n = 12$ , *R. radicans*  $2n = 10$ , *R. riparia*  $2n = 10$ , *R. pubera*  $2n = 10$ , *R. pubera*  $2n = 12$ , *R. brevisuscula*  $2n = 10$ , *R. colorata*  $2n = 10$ , *R. nervosa* subsp. *ciliata*  $2n = 10$ , *R. filiformis*  $2n = 10$ , *R. cephalotes*  $2n = 18$ , *R. tenerima*  $2n = 20$ , *R. tenuis*  $2n = 4$ , and *R. alba*  $2n = 26$ . Note that despite some similar patterns to those of *R. brevisuscula*, we could not decipher the complete karyotype of *R. pubera*-12. Bars = 5  $\mu$ m.

### SUPPLEMENTARY FIGURE 2

Chromosome identification in prometaphase cells by oligo-FISH barcoding in *R. pubera*-10 using Rbv-I (green) and Rbv-II (magenta) probes developed in *R. brevisuscula*. 8x4 green and 7x4 magenta signals are shown with a total of 60 signals in the haploid genome of *R. pubera*-10. Bar = 5  $\mu$ m.

- Liu, X., Sun, S., Wu, Y., Zhou, Y., Gu, S., Yu, H., et al. (2020). Dual-color oligo-FISH can reveal chromosomal variations and evolution in *Oryza* species. *Plant J.* 101 (1), 112–121. doi: 10.1111/tpj.14522
- Liu, G., and Zhang, T. (2021). Single copy oligonucleotide fluorescence *in situ* hybridization probe design platforms: development, application and evaluation. *Int. J. Mol. Sci.* 22 (13), 7124. doi: 10.3390/ijms22137124
- Lucek, K., Augustijnen, H., and Escudero, M. (2022). A holocentric twist to chromosomal speciation? *Trends Ecol. Evol.* 37, 655–662. doi: 10.1016/j.tree.2022.04.002
- Luo, X., Liu, J., and He, Z. (2022). Oligo-FISH can identify chromosomes and distinguish *Hippophaë rhamnoides* L. *Taxa. Genes* 13 (2), 195. doi: 10.3390/genes13020195
- Márquez-Corro, J. I., Martín-Bravo, S., Blanco-Pastor, J. L., Luceño, M., and Escudero, M. (2023). The holocentric chromosome microevolution: From phylogeographic patterns to genomic associations with environmental gradients. *Mol. Ecol.* 00, 1–13. doi: 10.1111/mec.17156
- Melters, D. P., Paliulis, L. V., Korf, I. F., and Chan, S. W. (2012). Holocentric chromosomes: convergent evolution, meiotic adaptations, and genomic analysis. *Chromosome Res.* 20, 579–593. doi: 10.1007/s10577-012-9292-1
- Meng, Z., Zhang, Z., Yan, T., Lin, Q., Wang, Y., Huang, W., et al. (2018). Comprehensively characterizing the cytological features of *Saccharum spontaneum* by the development of a complete set of chromosome-specific oligo probes. *Front. Plant Sci.* 9, 1624. doi: 10.3389/fpls.2018.01624
- Nascimento, T., and Pedrosa-Harand, A. (2023). High rates of structural rearrangements have shaped the chromosome evolution in dysploid *Phaseolus* beans. *Theor. Appl. Genet.* 136 (10), 1–14. doi: 10.1007/s00122-023-04462-3
- Parween, S., Nawaz, K., Roy, R., Pole, A. K., Venkata Suresh, B., Misra, G., et al. (2015). An advanced draft genome assembly of a desi type chickpea (*Cicer arietinum* L.). *Sci. Rep.* 5 (1), 12806. doi: 10.1038/srep12806
- POWO (2023). *Plants of the world online* (Kew: Facilitated by the Royal Botanic Gardens). Available at: <http://www.plantsoftheworldonline.org>.
- Qin, S., Wu, L., Wei, K., Liang, Y., Song, Z., Zhou, X., et al. (2019). A draft genome for *Spatholobus suberectus*. *Sci. Data* 6 (1), 113. doi: 10.1038/s41597-019-0110-x
- Ribeiro, T., Buddenhagen, C. E., Thomas, W. W., Souza, G., and Pedrosa-Harand, A. (2018). Are holocentrics doomed to change? Limited chromosome number variation in *Rhynchospora* Vahl (Cyperaceae). *Protoplasma* 255, 263–272. doi: 10.1007/s00709-017-1154-4
- Ribeiro, T., Marques, A., Novák, P., Schubert, V., Vanzela, A. L., Macas, J., et al. (2017). Centromeric and non-centromeric satellite DNA organisation differs in holocentric *Rhynchospora* species. *Chromosoma* 126, 325–335. doi: 10.1007/s00412-016-0616-3
- Ruban, A., Fuchs, J., Marques, A., Schubert, V., Soloviev, A., Raskina, O., et al. (2014). B chromosomes of *Aegilops speltoides* are enriched in organelle genome-derived sequences. *PLoS One* 9 (2), e90214. doi: 10.1371/journal.pone.0090214
- Schubert, V., Neumann, P., Marques, A., Heckmann, S., Macas, J., Pedrosa-Harand, A., et al. (2020). Super-resolution microscopy reveals diversity of plant centromere architecture. *Int. J. Mol. Sci.* 21 (10), 3488. doi: 10.3390/ijms21103488
- Senaratne, A. P., Cortes-Silva, N., and Drinnenberg, I. A. (2022). “Evolution of holocentric chromosomes: drivers, diversity, and deterrents,” in *Seminars in cell & Developmental biology* 127, 90–99. doi: 10.1016/j.semcdb.2022.01.003
- Silva Filho, P. J., Thomas, W. W., and Boldrini, I. I. (2021). Redefining *Rhynchospora* section *Tenuis* (Cyperaceae), a phylogenetic approach. *Bot. J. Linn. Soc.* 196 (3), 313–328. doi: 10.1093/botlinnean/boab002
- Thomas, W. W., Araújo, A. C., and Alves, M. V. (2009). A preliminary molecular phylogeny of the *Rhynchosporae* (Cyperaceae). *Bot. Rev.* 75, 22–29. doi: 10.1007/s12229-008-9023-7
- Vanzela, A. L. L. (1996). *Rhynchospora tenuis* Link (Cyperaceae): a species with the lowest number of holocentric chromosomes (n= 2). *Cytobios* 88, 219–228.
- Vanzela, A. L. L., and Colaço, W. (2002). Mitotic and meiotic behavior of  $\gamma$  irradiated holocentric chromosomes of *Rhynchospora pubera* (Cyperaceae). *Acta Sci.* 24 (2), 611–614. doi: 10.4025/actasciobiolsci.v24i0.2364
- Wong, C. Y. Y., Ling, Y. H., Mak, J. K. H., Zhu, J., and Yuen, K. W. Y. (2020). Lessons from the extremes: Epigenetic and genetic regulation in point monocentromere and holocentromere establishment on artificial chromosomes. *Exp. Cell Res.* 390 (2), 111974. doi: 10.1016/j.yexcr.2020.111974
- Yu, F., Chai, J., Li, X., Yu, Z., Yang, R., Ding, X., et al. (2021). Chromosomal characterization of *Triplidium arundinaceum* revealed by oligo-FISH. *Int. J. Mol. Sci.* 22 (16), 8539. doi: 10.3390/ijms22168539
- Zaki, N. M., Schwarzacher, T., Singh, R., Madon, M., Wischmeyer, C., Nor, N. H. M., et al. (2021). Chromosome identification in oil palm (*Elaeis guineensis*) using *in situ* hybridization with massive pools of single copy oligonucleotides and transferability across *Areaceae* species. *Chromosome Res.* 29, 373–390. doi: 10.1007/s10577-021-09675-0